ผลกระทบของ Knudsen Diffusion ต่อแบบจำลองของเซลล์เชื้อเพลิงชนิดเมมเบรนแลกเปลี่ยนโปรตอน

M. Hinaje[1], วัฒนา แก้วมณี[1,2], D. A. Nguyen[1], S. Rael[1] และ B. Davat[1]

บทคัดย่อ

ความเข้าใจในกลไกการทำงานของเซลล์เชื้อเพลิงเป็นสิ่งจำเป็นสำหรับการหาจุดการทำงานที่ดีที่สุดของเซลล์เชื้อเพลิงชนิดเมมเบรนแลกเปลี่ยนโปรตอน กลไกที่มีบทบาทสำคัญต่อการทำงานของเซลล์เชื้อเพลิงชนิดนี้คือการส่งผ่านแก๊สในชั้นแพร่กระจายแก๊สและการส่งถ่ายโปรตอนในเมมเบรน ชุดของสมการที่ซับซ้อนซึ่งต้องอาศัยต้นทุนการคำนวณมหาศาลเป็นสิ่งจำเป็นสำหรับการคำนวณที่ต้องการความถูกต้อง อย่างไรก็ดีสมการกลไกการแพร่กระจายแบบ Knudsen มักจะถูกละเลยเพื่อลดทอนความซับซ้อน

บทความนี้เป็นการศึกษาแบบจำลองชนิด 1 มิติ ของเซลล์เชื้อเพลิงชนิดเมมเบรนแลกเปลี่ยนโปรตอน ภายใต้เงื่อนไข isothermal และเมมเบรนถูกควบคุมความชื้น โดยได้ทำการเปรียบเทียบแบบจำลองหนึ่งซึ่งพิจารณาครอบคลุมถึงกลไกการแพร่กระจายแบบ Knudsen กับอีกแบบจำลองหนึ่งซึ่งละเลยผลจากกลไกการแพร่กระจายดังกล่าว ข้อมูลเชิงตัวเลขของปรากฏการณ์การส่งถ่ายแบบ Stefan-Maxwell และ Knudsen ซึ่งมีการเปลี่ยนแปลงตามค่าคุณสมบัติต่างๆของเมมเบรนได้ถูกนำเสนอในบทความนี้ ความต้านทานของเมมเบรนได้ถูกคำนวณจากแบบจำลองทั้งสองชนิด ซึ่งพบว่าการละเลยกลไกการแพร่กระจายแบบ Knudsen ทำให้ค่าความต้านทานของเมมเบรนที่ได้จากแบบจำลองทั้งสองต่างกันประมาณ 9% ซึ่งค่อนข้างมีนัยสำคัญ

คำสำคัญ : เซลล์เชื้อเพลิงชนิดเมมเบรนแลกเปลี่ยนโปรตอน, ความต้านทานของเมมเบรน

[1] Groupe de Recherche en Electrotechnique et Electronique de Nancy, Nancy-Universite, France

[2] อาจารย์ภาควิชาครุศาสตร์ไฟฟ้า คณะครุศาสตร์อุตสาหกรรม มหาวิทยาลัยเทคโนโลยีพระจอมเกล้าพระนครเหนือ
ผู้นิพนธ์ประสานงาน โทรศัพท์ 0-2913-2500 ต่อ 3302 E-mail : wattanak@kmutnb.ac.th

Knudsen Diffusion and Its Effect on PEM Fuel Cell Model

M. Hinaje[1], W. Kaewmanee[1,2], D. A. Nguyen[1], S. Rael[1] and B. Davat[1]

Abstract

With an aim of optimizing the operating points of the proton exchange membrane fuel cell (PEMFC), it is necessary to understand physical mechanisms of the cell. The physical mechanisms which play the important roles in the PEMFC are the gas transport in the gas diffusion layer and the proton transport in the membrane. Tremendous equations, which require massive computational cost, are used to describe the operations of the cell. However, the Knudsen diffusion, which is one kind of the transport mechanism in the fuel cell, is usually be neglected to reduce the computational cost.

This paper presents a comparative study between two types of one-dimensional (1-D) steady isothermal PEMFC models; one of which is include the effect of the Knudsen diffusion and the other one is not. The numerical results of the transport phenomena from both models have been presented. Membrane resistances from each case are computed to evaluate the effect of neglecting the Knudsen diffusion. The result has shown that neglecting the Knudsen diffusion causes about 9% relative error to the membrane resistances, which is quite significant.

Keyword: Proton exchange membrane fuel cell (PEMFC); membrane resistance

[1] Groupe de Recherche en Electrotechnique et Electronique de Nancy, Nancy-Universite, France

[2] Department of Teacher Training in Electrical Engineering, KMUTNB, Bangkok, Thailand

1. INTRODUCTION

Proton exchange membrane fuel cells (PEMFCs) are the devices that convert chemical energy into electrical energy. PEMFCs are believed to be the power sources for the electric vehicles in the future. The simplified structure of the PEMFC is shown in Fig. 1. The gas diffusion layers (GDL), the catalyst layers and the membrane are considered as the heart of the fuel cell. They are usually pressed together to become one unit. This unit is recognized as a membrane electrode assembly (MEA).

The electrical energy obtained from the PEMFCs is mainly depended on the chemical reactions and the transport phenomena in each part of the cell. There are mainly two kinds of the transport phenomena in the cell. One of them is the Stefan-Maxwell diffusion which represents the collision among gases molecules. The other one is Knudsen diffusions which represent the collision between gases molecules and porous wall of the fuel cell materials. However, the Knudsen diffusion is often vanished from the fuel cell model by the assumption that the mean free paths of gases molecules are much smaller than the pore size of the fuel cell material; i.e., the effect of molecule-molecule collision will dominate the total mass

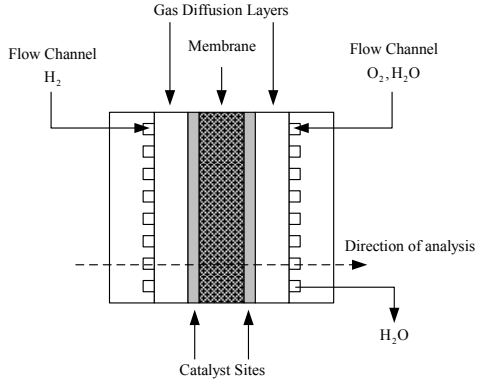

Fig. 1. A structure of a PEM single cell

TABLE I

NOMENCLATURE

a	Activity of water
Bo	Viscous flow parameter
C_i	Concentration of the species i ($mol.m^{-3}$)
D_{ij}^{eff}	Effective diffusion coefficient of water ($m^2.s^{-1}$)
D_{ik}	Knudsen diffusion ($m^2.s^{-1}$)
$D_{H_2O}^{m}$	Diffusion coefficient of water ($m^2.s^{-1}$)
d_p	Pore diameter of the GDLs (m)
EW	Equivalent weight ($kg.mol^{-1}$)
F	Faraday constant: 96485 ($C.mol^{-1}$)
I	Current (A)
J_{cell}	Current density ($A.m^{-2}$)
L_d	GDLs thickness (m)
L_m	Membrane thickness (m)
M_i	Molar mass of the species i ($kg.mol^{-1}$)
nd	Electro-osmotic drag coefficient
P_i	Partial pressure of species i (Pa)
P_i^*	Partial pressure of H_2, O2 at the cell entry ($mol.m^{-3}$)
P_{sat}	Saturated pressure (Pa)
P_T	Total pressure ($P_T = \sum P_i$) (Pa)
R	Universal gas constant, 8,314 J. $mol^{-1}K^{-1}$
$RH^{a,c}$	Anodic and cathodic relative humidity (%)
R_m	Membrane resistance ($\Omega.m^2$)
T	Temperature (K)
y_i	Molar fraction of species i (-)
z	Length (m)
Greek symbols	
ε	Dry porosity of the electrode
α	Charge transfer coefficient
$\eta^{a,c}$	Coefficient of viscosity of the gas mixture
λ	Water content (-)
ρ_{dry}	Membrane density ($kg.m^{-3}$)
σ_{H^+}	Protonic conductivity ($S.m^{-1}$)
τ	Tortuosity

Subscript

i	Components, H_2, O_2, H_2O, and N_2
v	Vapour water
l	Liquid water
w	Water

Superscript

a	Anode
c	Cathode
e	Entry
m	Membrane
prod	Produced

transport phenomena. The main reason for this assumption is to have a simpler model which reduces the computational cost when applied to the finite element computing machine. As the assumption has made, the model trade their accuracy with their simplicity. So that, it is interesting to observe the difference that the neglecting has made.

This research investigates the effect of neglecting the Knudsen diffusion effect by compares two types of one-dimension (1-D) models of the MEA where one of which neglect the Knudsen diffusion and the other one take Knudsen diffusion into account.

2. TRANSPORT PROCESS IN FUEL CELL

The fundamental operation of the fuel cell can be described as follows. At the anode side, the hydrogen, which is the fuel of the cell, diffuses through the anode diffusion layer to the catalyst site. The oxidation occurred at this site, where a hydrogen atom loses two electrons (1) and the remainder which considered as protons become part of hydronium ions $H3O^+$ (here simply refer to as proton or H^+). The proton immerses into the

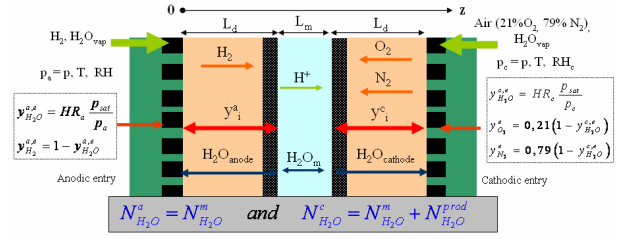

Fig. 2. Schematic representation of the gas flows in the fuel cell

$$H_2 \rightarrow 2H^+ + 2e^- \quad (1)$$

$$\frac{1}{2}O_2 + 2H^+ + 2e^- \rightarrow H_2O \quad (2)$$

membrane and the electrons, which provide useful electrical power, flow through an external circuit and return to the cathode side. In the meantime, proton travels through the membrane to the cathode side where an oxygen atom reacts with two protons and two electrons, which result in water and heat (2).

The MEA models presented here are 1-D steady state models. The models represent the coupled transport process in GDLs, catalyst layers, and a membrane. These models assume that:

- water exists only in the gas phase at the electrodes, and as solute water in membrane. The single phase model described here is sufficient for modeling the mass transport up to medium-high current densities [1], [2];
- cell temperature remains constant and homogeneous throughout the cell;
- catalyst layers are very thin and are considered as reactive surfaces ;
- membrane is gas-tight;
- current density across the MEA surface is homogeneous.

A. Transport in the GDLs

The fuel cell is usually fed by dry or humidified hydrogen and air. The gas diffusion region of thickness L_d begin at z = 0 on the anode side (or at z = (2 Ld)+Lm on the cathode side) and reaches the boundary at the point z = Ld (or at z = Ld + Lm).

At the anode and cathode GDL entries, the partial pressure of each species is given by

$$P^{a}_{H_2}(z=0) = P^{a}_{T} - RH^{a}\, P_{sat} \quad (3)$$

$$P^{a}_{H_2O}(z=0) = RH^{a}\, P_{sat} \quad (4)$$

$$P^{c}_{O_2}(z=2L_d+L_m) = 0.21 * P^{c}_{T} - RH^{c}\, P_{sat} \quad (5)$$

$$P^{c}_{N_2}(z=2L_d+L_m) = 0.79 * P^{c}_{T} - RH^{c}\, P_{sat} \quad (6)$$

$$P^{c}_{H_2O}(z=2L_d+L_m) = RH^{c}\, P_{sat} \quad (7)$$

In the above equations, the saturation pressure varies with temperature and can be calculated using the empirical expression [3]:

$$\mathrm{Log}_{10}P_{sat} = -2.1794 + 0.02953T - 9.1837(10^{-5})T^{2} + 1.4454(10^{-7})T^{3} \quad (8)$$

1) Stefan-Maxwell and Knudsen diffusion

For gas diffusions in porous media, the mean free path determines the significance of collision between gas molecules and the porous wall. The Stefan-Maxwell diffusion dominates the total diffusion when the pore diameter is bigger than one hundred times of the mean free path, while Knudsen diffusion dominates the total diffusion when the pore diameter is smaller than a tenth of the mean free path. Any pore diameter between these two limits will have the combined effect of both Knudsen and Stefan-Maxwell diffusion [4]. Combining Knudsen and Stefan-Maxwell diffusions together, the equations for mixture of each species are [5]:

$$-\frac{\vec{\nabla}P_i^{a,c}}{RT} = \frac{1}{D_{ik}^{eff}}\left[N_i^{a,c} + y_i^{a,c}\left(\frac{P_T^{a,c}}{RT}\frac{B_o}{\eta^{a,c}}\right)\vec{\nabla}P_T^{a,c}\right] + \sum_{\substack{j=1\\ i\neq j}}^{e}\frac{1}{D_{ij}^{eff}}\left(y_j^{a,c}N_i^{a,c} - y_i^{a,c}N_j^{a,c}\right) \quad (9)$$

With

$$\sum y_i^{a,c} = 1 \quad (10)$$

$$y_i^{a,c} = \frac{P_i^{a,c}}{P_T^{a,c}} \quad (11)$$

$$\sum P_i^{a,c} = P_T^{a,c} \quad (12)$$

The pressure of the mixture P_T is evaluated with the assumption of ideal and adiabatic gas.

Nitrogen takes no part in the reaction; hence its flux is equal to zero:

$$N^{c}_{N_2} = 0 \quad (13)$$

From mass conservation equation:

$$\frac{1}{RT}\frac{\partial P_i^{a,c}}{\partial t} + \vec{\nabla}.N_i^{a,c} = 0\,. \quad (14)$$

As this is the steady-state analysis, $\partial P_i^{a,c} / \partial t = 0$, therefore $\vec{\nabla}.N_i^{a,c} = 0$, i.e. the flux of the considered species $N_i^{a,c}$ is constant.

The inlet mixture gas is constituted by two species in the anode, which are H_2 and H_2O, and three species in the cathode, which are O_2, N_2, and H_2O. Thus, with the assumptions listed above and replacing P_T by the sum of the partial pressures (12), and the molar fraction by its expression given in (11), the diffusion equations in the anode and cathode can be rewritten as:

In anode,

$$\frac{\partial P^a_{H_2}}{\partial z}\left(P^a_{H_2}+P^a_{H_2O}\right)\left(1+P^a_{H_2}\frac{B_O}{D_{H_2,k}\eta^a}\right)+\frac{\partial P^a_{H_2O}}{\partial z}\left(P^a_{H_2}+P^a_{H_2O}\right)P^a_{H_2}\frac{B_O}{D_{H_2,k}\eta^a}$$
$$=P^a_{H_2}RT\left(\frac{N^a_{H_2O}}{D^{eff}_{H_2-H_2O}}-\frac{N^a_{H_2}}{D_{H_2,k}}\right)-P^a_{H_2O}RT\,N^a_{H_2}\left(\frac{1}{D^{eff}_{H_2-H_2O}}+\frac{1}{D_{H_2,k}}\right) \quad (15)$$

$$\frac{\partial P^a_{H_2O}}{\partial z}\left(P^a_{H_2}+P^a_{H_2O}\right)\left(1+P^a_{H_2O}\frac{B_O}{D_{H_2O,k}\eta^a}\right)+\frac{\partial P^a_{H_2}}{\partial z}\left(P^a_{H_2}+P^a_{H_2O}\right)P^a_{H_2O}\frac{B_O}{D_{H_2O,k}\eta^a}$$
$$=P^a_{H_2O}RT\left(\frac{N^a_{H_2}}{D^{eff}_{H_2O-H_2}}-\frac{N^a_{H_2O}}{D_{H_2O,k}}\right)-P^a_{H_2}RT\,N^a_{H_2O}\left(\frac{1}{D^{eff}_{H_2O-H_2}}+\frac{1}{D_{H_2O,k}}\right) \quad (16)$$

In cathode,

$$\frac{\partial P^c_{O_2}}{\partial z}\left(P^c_{O_2}+P^c_{N_2}+P^c_{H_2O}\right)\left(1+P^c_{O_2}\frac{B_O}{D_{O_2,k}\eta^c}\right)+$$
$$\left(\frac{\partial P^c_{N_2}}{\partial z}+\frac{\partial P^c_{H_2O}}{\partial z}\right)\left(P^c_{O_2}+P^c_{N_2}+P^c_{H_2O}\right)P^c_{O_2}\frac{B_O}{D_{O_2,k}\eta^c}=$$
$$P^c_{O_2}RT\left(\frac{N^c_{N_2}}{D^{eff}_{O_2-N_2}}+\frac{N^c_{H_2O}}{D^{eff}_{O_2-H_2O}}-\frac{N^c_{O_2}}{D_{O_2,k}}\right)$$
$$-P^c_{N_2}RT\,N^c_{O_2}\left(\frac{1}{D^{eff}_{O_2-N_2}}+\frac{1}{D_{O_2,k}}\right)-P^c_{H_2O}RT\,N^c_{O_2}\left(\frac{1}{D^{eff}_{O_2-H_2O}}+\frac{1}{D_{O_2,k}}\right) \quad (17)$$

$$\frac{\partial P^c_{N_2}}{\partial z}\left(P^c_{O_2}+P^c_{N_2}+P^c_{H_2O}\right)\left(1+P^c_{N_2}\frac{B_O}{D_{N_2,k}\eta^c}\right)+$$
$$\left(\frac{\partial P^c_{O_2}}{\partial z}+\frac{\partial P^c_{H_2O}}{\partial z}\right)\left(P^c_{O_2}+P^c_{N_2}+P^c_{H_2O}\right)P^c_{N_2}\frac{B_O}{D_{N_2,k}\eta^c}=$$
$$P^c_{N_2}RT\left(\frac{N^c_{O_2}}{D^{eff}_{N_2-O_2}}+\frac{N^c_{H_2O}}{D^{eff}_{N_2-H_2O}}-\frac{N^c_{O_2}}{D_{O_2,k}}\right)$$
$$-P^c_{O_2}RT\,N^c_{N_2}\left(\frac{1}{D^{eff}_{N_2-O_2}}+\frac{1}{D_{N_2,k}}\right)-P^c_{H_2O}RT\,N^c_{N_2}\left(\frac{1}{D^{eff}_{N_2-H_2O}}+\frac{1}{D_{N_2,k}}\right) \quad (18)$$

$$\frac{\partial P^c_{H_2O}}{\partial z}\left(P^c_{O_2}+P^c_{N_2}+P^c_{H_2O}\right)\left(1+P^c_{H_2O}\frac{B_O}{D_{H_2O,k}\eta^c}\right)+$$
$$\left(\frac{\partial P^c_{O_2}}{\partial z}+\frac{\partial P^c_{N_2}}{\partial z}\right)\left(P^c_{O_2}+P^c_{N_2}+P^c_{H_2O}\right)P^c_{H_2O}\frac{B_O}{D_{H_2O,k}\eta^c}$$
$$=P^c_{H_2O}RT\left(\frac{N^c_{N_2}}{D^{eff}_{O_2-N_2}}+\frac{N^c_{O_2}}{D^{eff}_{H_2O-O_2}}-\frac{N^c_{H_2O}}{D_{H_2O,k}}\right)$$
$$-P^c_{N_2}RT\,N^c_{H_2O}\left(\frac{1}{D^{eff}_{H_2O-N_2}}+\frac{1}{D_{H_2O,k}}\right)-P^c_{O_2}RT\,N^c_{H_2O}\left(\frac{1}{D^{eff}_{H_2O-O_2}}+\frac{1}{D_{H_2O,k}}\right) \quad (19)$$

The interactions between a pair of species (i,j) are characterized by the binary diffusion coefficient [6] :

$$D_{ij}=D^0_{ij}\left(P^0,T^0\right)\frac{P^0}{T^0}\left(\frac{T}{T^0}\right)^{\frac{3}{2}} \quad (20)$$

The effective diffusion coefficients which incorporate the effect of the GDLs porosity are described by Bruggeman relation:

$$D^{eff}_{ij}=D_{ij}\varepsilon^{\frac{3}{2}} \quad (21)$$

Using the Onsager reciprocal relation [7], [8], we also have:

$$D^{eff}_{ij}=D^{eff}_{ji} \quad (22)$$

$D_{i,k}$ is the effective diffusion coefficient between species i and the porous medium. The $D_{i,k}$ are known to be independent of pressure and composition because the species behave independently in low pressure Knudsen regime [9].

$$D_{i,k}=\frac{d_p}{3}\sqrt{\frac{8RT}{\pi M_i}} \quad (23)$$

where d_p is the pore diameter and M_i is the molar mass of the specie i.

The last parameter needed for the porous medium model is the viscous-flow parameter B_o which is given by the following relation [9]:

$$B_o = \frac{\varepsilon}{\tau}\frac{(d_p)^2}{24} \tag{24}$$

where ε/τ is the porosity-tortuosity factor of the porous medium.

2) Neglecting the Knudsen diffusion

From the preceded section, we add the hypothesis that the Knudsen diffusion has very small effect to the total diffusion compared to the Stefan-Maxwell diffusion. So that, we can neglect the Knudsen diffusion terms from the preceded model as follow [10]:

In anode,

$$\frac{\partial P^a_{H_2}}{\partial z}\left(P^a_{H_2}+P^a_{H_2O}\right)=P^a_{H_2}RT\left(\frac{N^a_{H_2O}}{D^{eff}_{H_2-H_2O}}\right)-P^a_{H_2O}RT\,N^a_{H_2}\left(\frac{1}{D^{eff}_{H_2-H_2O}}\right) \tag{25}$$

$$\frac{\partial P^a_{H_2O}}{\partial z}\left(P^a_{H_2}+P^a_{H_2O}\right)=P^a_{H_2O}RT\left(\frac{N^a_{H_2}}{D^{eff}_{H_2O-H_2}}\right)-P^a_{H_2}RTN^a_{H_2O}\left(\frac{1}{D^{eff}_{H_2O-H_2}}\right) \tag{26}$$

In cathode,

$$\frac{\partial P^c_{O_2}}{\partial z}\left(P^c_{O_2}+P^c_{N_2}+P^c_{H_2O}\right)=P^c_{O_2}RT\left(\frac{N^c_{N_2}}{D^{eff}_{O_2-N_2}}+\frac{N^c_{H_2O}}{D^{eff}_{O_2-H_2O}}\right)-P^c_{N_2}RT\left(\frac{N^c_{O_2}}{D^{eff}_{O_2-N_2}}\right)-P^c_{H_2O}RT\left(\frac{N^c_{O_2}}{D^{eff}_{O_2-H_2O}}\right) \tag{27}$$

$$\frac{\partial P^c_{N_2}}{\partial z}\left(P^c_{O_2}+P^c_{N_2}+P^c_{H_2O}\right)=P^c_{N_2}RT\left(\frac{N^c_{O_2}}{D^{eff}_{N_2-O_2}}+\frac{N^c_{H_2O}}{D^{eff}_{N_2-H_2O}}\right)-P^c_{O_2}RT\left(\frac{N^c_{N_2}}{D^{eff}_{N_2-O_2}}\right)-P^c_{H_2O}RT\left(\frac{N^c_{N_2}}{D^{eff}_{N_2-H_2O}}\right) \tag{28}$$

$$\frac{\partial P^c_{H_2O}}{\partial z}\left(P^c_{O_2}+P^c_{N_2}+P^c_{H_2O}\right)=P^c_{H_2O}RT\left(\frac{N^c_{N_2}}{D^{eff}_{O_2-N_2}}+\frac{N^c_{O_2}}{D^{eff}_{H_2O-O_2}}\right)-P^c_{N_2}RT\left(\frac{N^c_{H_2O}}{D^{eff}_{H_2O-N_2}}\right)-P^c_{O_2}RT\,N^c_{H_2O}\left(\frac{N^c_{H_2O}}{D^{eff}_{H_2O-O_2}}\right) \tag{29}$$

The above system is then coupled to the membrane transport as shown in fig. 2. The equations for the membrane transport will be discussed in the next section.

B. Transport in the membrane

1) Water transport

The water transport in the membrane is governed by two competing diffusion mechanisms. One is due to the proton displacement from anode to cathode which drags some water molecules with them; this phenomenon is called electro-osmotic drag. The other mechanism is back diffusion of water from cathode to anode. This back diffusion is a result of the water concentration gradient created in the membrane by the electro-osmotic drag and the water produced by the chemical reaction at the cathode.

Therefore, the total mass flux of water transported inside the membrane is given by [11]:

$$N^m_{H_2O} = n_d\frac{j_{cell}}{F} - D^m_{H_2O}\frac{dc_{H_2O}}{dz} \tag{30}$$

where $D^m_{H_2O}$ is the diffusion coefficient of water which calculated by Fuller and Newman [12] as follow:

$$D^m_{H_2O} = \left(2.1\ 10^{-7}\right)\lambda\exp\left(-\frac{2436}{T}\right) \tag{31}$$

The drag coefficient, n_d, for Gore membranes is about unity [13], [14].

Water concentration in the membrane, c_{H2O} (mol/m^3), is defined by using the equivalent weight EW (kg.mol^{-1} SO_3), the dry membrane density, ρ_{dry} (kg.m^{-3}), and the water content [4]:

$$c_{H_2O} = \frac{\rho_{dry}}{EW}\lambda \tag{32}$$

Substituting (32) into (30) yields the total water flux as a function of water content λ

$$N^m_{H_2O} = n_d \frac{j_{cell}}{F} - D^m_{H_2O}\frac{\rho_{dry}}{EW}\frac{d\lambda}{dz} \tag{33}$$

The relation in (33) can be expressed as:

$$dz = \frac{F\rho_{dry}}{EW}\frac{D^m_{H_2O}}{n_d j_{cell} - F N^m_{H_2O}}d\lambda \tag{34}$$

The correct parameter should satisfy:

$$L_m = \frac{F\rho_{dry}}{EW}\int_{\lambda_a}^{\lambda_c}\frac{D^m_{H_2O}}{n_d j_{cell} - F N^m_{H_2O}}d\lambda \tag{35}$$

2) Water content in the membrane

To integrate (35), the water content at the membrane/electrode interfaces, λ_c and λ_a must be known. The relation of the water content with the surrounding medium is given by water uptake measured at different temperatures [15].

Water content of the membrane can be estimated from the surrounded vapour activity, a, by Springer's method [16] which is shown in (36), (37). However, water content information from Springer's experimental is available only at 30°C and 80°C. The estimated water contents between these two temperatures can be obtained by linear interpolations [16].

$$\lambda_{80^\circ} = 0.3 + 10.8a - 16a^2 + 14.1a^3 \tag{36}$$

$$\lambda_{30^\circ} = \begin{cases} 0.043 + 17.81a - 39.85a^2 + 36a^3 & 0 < a < 1 \\ 14 + 1.4(a-1) & 1 \le a \le 3 \\ 16.8 & a > 3 \end{cases} \tag{37}$$

The activities at the anode-electrode/membrane interface, a_a, and at the cathode-electrode /membrane interface, a_c, can be calculated as follow:

$$a_a = y^a_{H_2O}\frac{P}{P_{sat}(T)} \tag{38}$$

$$a_c = y^c_{H_2O}\frac{P}{P_{sat}(T)} \tag{39}$$

C. Electrode membrane interfaces

At the membrane/electrodes interface, the continuity of water flux density is defined as:

$$N^a_{H_2O} = N^m_{H_2O} \text{ at } z = L_d \tag{40}$$

$$N^c_{H_2O} = N^m_{H_2O} + N^{pro}_{H_2O} \text{ at } z = L_d + L_m \tag{41}$$

where $N^{pro}_{H_2O}$ is the water produced by the redox reaction. For a given load current density j_{cell}, the gas consumptions and the water produced are equal to:

$$N_{O_2} = -\frac{j_{cell}}{4F} \quad \text{on } z = L_d + L_m \tag{42}$$

$$N_{H_2} = \frac{j_{cell}}{2F} \quad \text{on } z = L_d \tag{43}$$

$$N^{pro}_{H_2O} = \frac{j_{cell}}{2F} \quad \text{on } z = L_d + L_m \tag{44}$$

D. Membrane resistance

As the membrane resistance depends on the humidification state of the fuel cell, one can say the conductivity of the membrane [16] is related to the

water content of the membrane. Increasing of water content in the membrane (PEMFC well humidified) will result in the increasing of the membrane conductivity and decreasing of the membrane resistance.

$$R_m = \int_{L_d}^{L_d+L_m} \frac{1}{\sigma_{H^+}(z)} dz \, , \, [\Omega.m^2] \qquad (45)$$

where σ_{H^+} is the membrane conductivity and expressed as follow:

$$\sigma_{H^+} = (0.5139\lambda - 0.326) e^{1268\left(\frac{1}{303} - \frac{1}{T}\right)} \quad \text{for } \lambda > 1 \qquad (46)$$

If λ is less than 1, the ionic conductivity is assumed constant [18].

3. RESULTS AND DISCUSSION

In this part, we will first show the influence of the porosity and the pore size on the molar fractions and on the water flux in the membrane. The simulations will be made for different porosity from 0.3 to 0.6 and for various radius pore sizes from $5\,\mu m$ to $15\,\mu m$. Table II shows the simulation parameters.

A. Influence of the porosity

The diffusion of oxygen and water are plotted along the GDLs when fixing the radius pore to $10\,\mu m$.

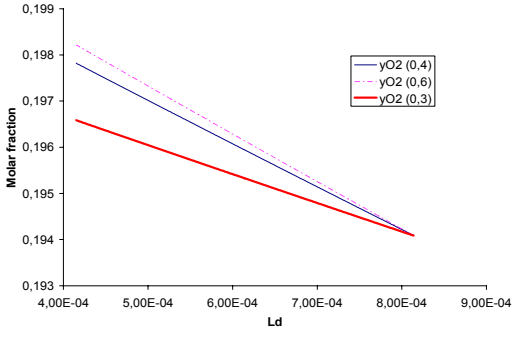

Fig. 3. Oxygen molar fraction along the GDL without Knudsen diffusion effect

TABLE II

SIMULATION PARAMETER

Anode and Cathode	
operating pressure (atm)	1
Cell temperature (°C)	50
Rha(%)	0
Rhc(%)	65
Lm (10^{-6} m)	15
Ld (10^{-6} m)	400
EW (kg.mol^{-1})	0.95
ρ_{dry} (kg.m^{-3})	2020
η^a (10^{-6} m)	8,61
η^c (10^{-6} m)	19,52
τ	$\pi/2$
I (A)	10

* depends on the temperature and the relative humidity of the inlet gas.

The O_2 molar fraction at the membrane/cathode interface increases with the porosity with both models as it can be seen in Fig. 3 and 4. However, a difference can be noticed on the variation of the molar fraction along the gas diffusion layer. As the Knudsen diffusion is neglected, the molar fraction increases linearly with the distance, which is not the case in Fig. 4 as we can see a non-linear profile of O_2 along the diffusion distance.

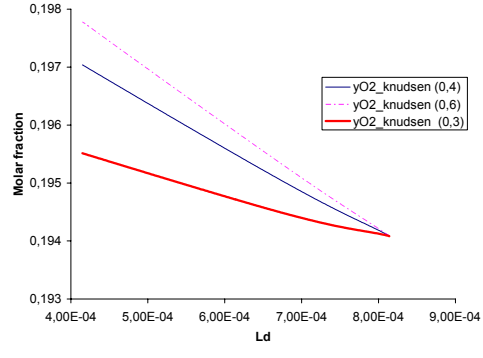

Fig. 4. Oxygen molar fraction along the GDL with Knudsen diffusion effect

If we compare the oxygen and water molar fractions computing with the both models, we can notice in Fig. 5 that the Knudsen diffusion allowed less molecules of oxygen to reach the membrane/electrode interface (we can see the same effect with H_2). Since the sum of the molar fraction is equal to unity, if the oxygen molar fraction decreases the vapor molar fraction will increases as shown in Fig. 6 and 7. The increasing of vapor molar fraction at the membrane/electrode interfaces affects the water content of the membrane as shown in Fig. 8, and then, results in the decreasing of the membrane resistance.

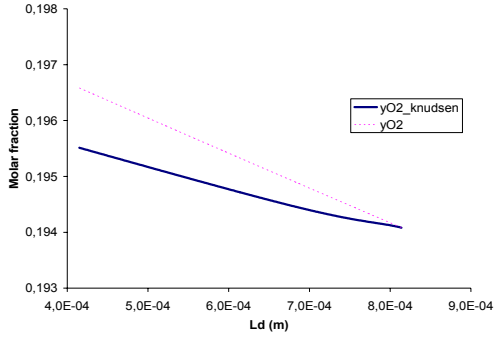

Fig. 5. Oxygen molar fraction ($\varepsilon = 0.3$) with and without Knudsen diffusion

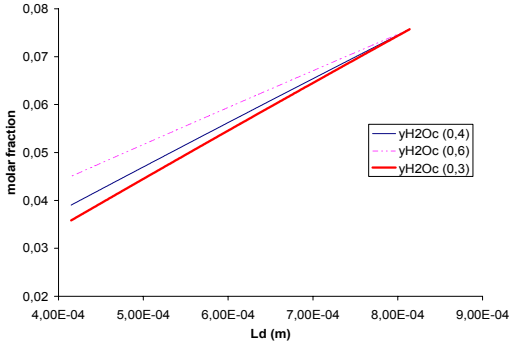

Fig. 6. Water molar fraction diffusion along the GDL without Knudsen diffusion effect

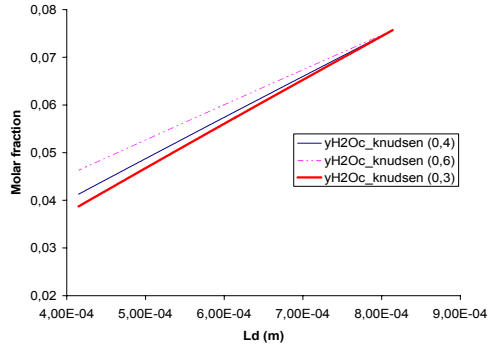

Fig. 7. Water molar fraction diffusion along the GDL with Knudsen diffusion effect

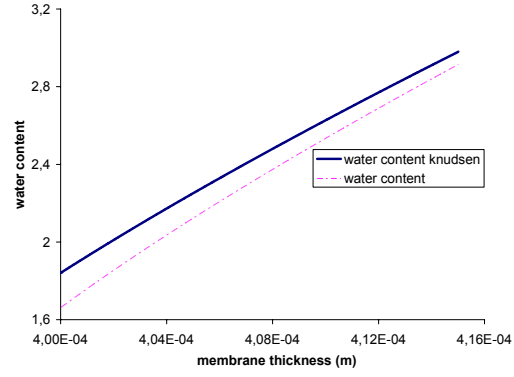

Fig. 8. Water content of the membrane with and without Knudsen diffusion ($\varepsilon = 0.3$)

B. Influence of the radius of the pore size

The pore sizes parameter is appeared only in the model that incorporated the Knudsen diffusion effect. The following numerical results are obtained by using the data given in table 1 and with $\varepsilon = 0.3$. As one can expect, the O_2 molar fraction at the cathode membrane interface is varied according to the radius of the pore size.

Water profiles are also affected by the radius of the pore size and eventually influence the membrane resistance as shown in Fig. 11.

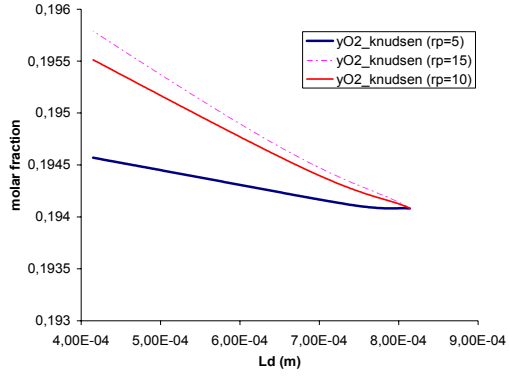

Fig. 9. Diffusion of O_2 along the gas diffusion layer for different pore size ($\varepsilon = 0.3$)

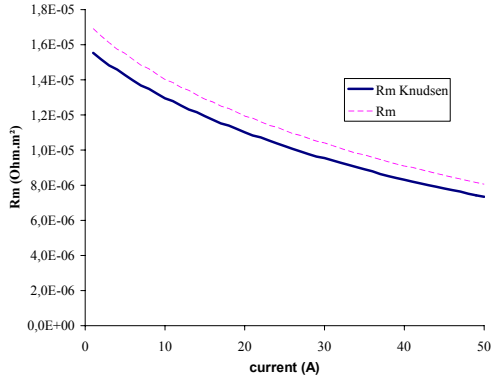

Fig. 12. Stack membrane resistance with and without Knudsen diffusion ($\varepsilon = 0.3$, r_p=10 μm)

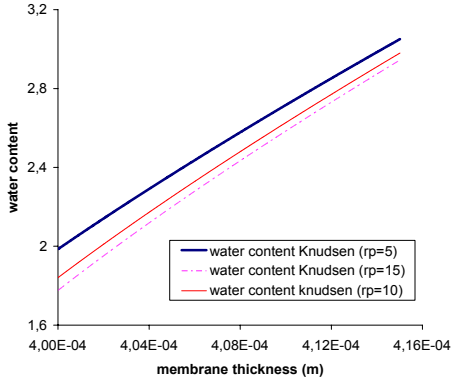

Fig. 10. Water content of the membrane for different pore size ($\varepsilon = 0.3$)

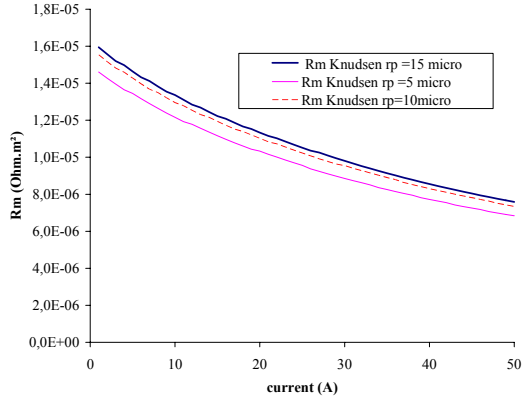

Fig. 11. Stack membrane resistance versus current

By comparing the membrane resistance computed with both models, we can highlight that the two curves are not close to each other. The study shows that neglecting the effect of Knudsen diffusion can lead to about 9% relative error on the membrane resistance value which is quite significant.

4. CONCLUSION

In this paper the 1-D simulations for a steady, isothermal, humidified PEM fuel cell have been made. The simulation pays particular attention to the transport phenomena occurred in the gas diffusion layers and the membrane. Various effects from varying parameter such as porosity or radius of pore size have been shown. The simulation results show that the simplification by neglecting the Knudsen diffusion effect introduces about 9% of relative error to the membrane resistance which is quite significant. Then, if a high precision for the membrane resistance is needed, the Knudsen diffusion effect should not be removed from the model.

REFERENCES

[1] M. Hu, A. Gu, M. Wang, X. Zhu, L. Yu, Three dimensional, two phase flow mathematical model for PEM fuel cell: Part I. Model development, Energy Conversion and Management 45 (2004), pp.1861-1882.

[2] M. Hu, A. Gu, M. Wang, X. Zhu, L. Yu, Three dimensional, two phase flow mathematical model for PEM fuel cell: Part II. Analysis and discussion of the internal transport mechanisms, Energy Conversion and Management 45 (2004), pp.1883-1916.

[3] M.-S. Chiang, and H.-S. Chu, Numerical investigation of transport component design effect on a proton exchange membrane fuel cell, Journal of Power Sources 160 (2006), pp.340-352.

[4] W. A. Philipp, J. Rzayev, M. A. Hillmyer, E. L. Cussler, Gas and water liquid transport through nanoporous block copolymer membranes, Journal of Membrane science 286 (2006), pp.144-152.

[5] Thampan, T., Malhotra, S., Tang, H. and R. Datta. "Modeling of conductive transport in proton-exchange membranes for fuel cells." Journal of The Electrochemical Society 147 (2000), pp.3242-3250

[6] M. F. Serincan, and S. Yesilyurt. “Transient Analysis of PEMFC at Start-Up and Failure”, Fuel cell 2, (2006), pp.118-127.

[7] M. H. Daneshpajooh, E. A. Mason, E. H. Bresler and R. P. Wendt, Equation for membrane transport, Biophysical journal 15 (1975), pp.591-613.

[8] C. W. Monroe and J. Newman, Onsager reciprocal relations for Stefan-Maxwell diffusion, American chemical Society 45 (2006), pp.5361-5367.

[9] E. A Mason, A. P. Malinauska, Gas Transport in Porous media: The dusty-Gas model, Elsevier Science Publishers, 1983, chap.2.

[10] Hirschfelder, J.O, C. F. Curtiss, R. B. Bird, “Molecular theory of gases and liquids”, John Wiley&Sons, New York, 1964, chap. 8.

[11] P. Berg, K. Promislow, J. St Pierre, J. Stumper, B. Wetton, Water managemet in PEM fuel cells, J. Electrochem. Soc. 151 (2004), pp.A341-A353.

[12] T. F. Fuller and J. Newman, Water and thermal management in solid-polymer-electrolyte fuel cells, J. Electrochem. Soc. 140 (1993), pp.1218-1225,.

[13] F. Liu, G.lu, and C.-Y. Wang, Water transport coefficient distribution through the membrane in polymer electrolyte fuel cell, J. Membrane Science 287 (2007), pp.126-131.

[14] X. Ye, C. Y. Wang, Measurements of water transport properties through membrane electrode assemblies. Part I membranes, J. Electrochem. Soc. (2007), pp.B676-B682.

[15] T. E. Springer, T. A. Zawodzinski, M. S Wilson and S. Gottesfeld, “Characterization of Polymer Electrolyte Fuel Cells Using AC Impedance Spectroscopy”, J. Electrochem. Soc., Vol. 143, (1996), pp.587-599.

[16] T. E. Springer, T. A. Zawodzinski and S. Gottesfeld, Polymer Electrolyte Fuel Cell Model, J. Electrochem. Soc. 138, (1991), pp. 2334-2342.

[17] J. Hinatsu, M. Mizuhata, and H. Takenaka. Water uptake of perfluorosulfonic acid membranes from liquid water and water vapour, Journal of the Electrochemical Society 141 (1994), pp.1493 -1498.

[18] S. H. Ge, and B.-L. Yi, A mathematical model for PEMFC in different flow modes, Journal of Power Sources 124 (2003), pp.1-11.